Original Article

BCKDK alters the metabolism of non-small cell lung cancer

Yanhui Wang[1#], Jiawei Xiao[1#], Wenna Jiang[1], Duo Zuo[1], Xia Wang[2], Yu Jin[1], Lu Qiao[1], Haohua An[1], Lexin Yang[1], Daphne W. Dumoulin[3], Wolfram C. M. Dempke[4], Sarah A. Best[5,6], Li Ren[1]

[1]Department of Clinical Laboratory, Tianjin Medical University Cancer Institute and Hospital, National Clinical Research Center for Cancer, Key Laboratory of Cancer Prevention and Therapy, Tianjin's Clinical Research Center for Cancer, Tianjin, China; [2]Department of Gastroenterology, Tianjin Medical University Cancer Institute and Hospital, Tianjin, China; [3]Department of Pulmonary Diseases Erasmus MC, Erasmus MC Cancer Institute, Rotterdam, The Netherlands; [4]Department of Haematology and Oncology, University of Munich, Munich, Germany; [5]Personalized Oncology Division, The Walter and Eliza Hall Institute of Medical Research, Parkville, Australia; [6]Department of Medical Biology, The University of Melbourne, Melbourne, Australia

Contributions: (I) Conception and design: Y Wang, L Ren; (II) Administrative support: W Jang, Y Wang; (III) Provision of study materials or patients: D Zuo, X Wang; (IV) Collection and assembly of data: J Xiao, Y Jin; (V) Data analysis and interpretation: J Xiao, H An, L Qiao; (VI) Manuscript writing: All authors; (VII) Final approval of manuscript: All authors.

[#]These authors contributed equally to this work.

Correspondence to: Li Ren. Department of Clinical Laboratory, Tianjin Medical University Cancer Institute and Hospital, National Clinical Research Center for Cancer, Key Laboratory of Cancer Prevention and Therapy, Tianjin's Clinical Research Center for Cancer, Tianjin 300060, China. Email: liren@tmu.edu.cn.

Background: Metabolic reprogramming is a major feature of many tumors including non-small cell lung cancer (NSCLC). Branched-chain α-keto acid dehydrogenase kinase (BCKDK) plays an important role in diabetes, obesity, and other diseases. However, the function of BCKDK in NSCLC is unclear. This study aimed to explore the function of BCKDK in NSCLC.

Methods: Metabolites in the serum of patients with NSCLC and the supernatant of NSCLC cell cultures were detected using nuclear magnetic resonance (NMR) spectroscopy. Colony formation, cell proliferation, and cell apoptosis were assessed to investigate the function of BCKDK in the progression of NSCLC. Glucose uptake, lactate production, cellular oxygen consumption rate, extracellular acidification rate, and reactive oxygen species (ROS) were measured to examine the function of BCKDK in glucose metabolism. The expression of BCKDK was measured using reverse transcriptase-polymerase chain reaction, western blot, and immunohistochemical assay.

Results: Compared with healthy controls and postoperative NSCLC patients, increased branched-chain amino acid (BCAA) and decreased citrate were identified in the serum of preoperative NSCLC patients. Upregulation of BCKDK affected the metabolism of BCAAs and citrate in NSCLC cells. Knockout of BCKDK decreased the proliferation and exacerbated apoptosis of NSCLC cells ex vivo, while increased oxidative phosphorylation and, ROS levels, and inhibited glycolysis.

Conclusions: BCKDK may influence glycolysis and oxidative phosphorylation by regulating the degradation of BCAA and citrate, thereby affecting the progression of NSCLC.

Keywords: Branched-chain α-keto acid dehydrogenase kinase (BCKDK); branched-chain amino acids (BCAAs); citrate; non-small cell lung cancer (NSCLC); glucose metabolism

Submitted May 15, 2021. Accepted for publication Dec 08, 2021.
doi: 10.21037/tlcr-21-885
View this article at: https://dx.doi.org/10.21037/tlcr-21-885

Introduction

Lung cancer, especially non-small cell lung cancer (NSCLC), is the most common cancer and the leading cause of cancer-related death, accounting for over 1.7 million deaths worldwide in 2020 (1). Most patients are diagnosed at an advanced stage, and early diagnosis and treatment of NSCLC remain an unmet need (2).

The alteration of tumor metabolism is closely related to the occurrence and progression of tumors (3). Tumor metabolism is generally characterized by increased lactic acid levels and decreased glutamine levels in blood circulation, and key enzymes in the metabolism of these substances have emerged as potential therapeutic targets (4). The advancement of metabolomics technology has led to the discovery of new and valuable differentially abundant metabolite (5-9), such as branched-chain amino acids (BCAAs). Elevated circulating levels of BCAAs have been linked to type 2 diabetes mellitus (10), insulin resistance (11) and Huntingtons disease (12). The importance of BCAA metabolic rewiring has been recently identified in multiple human cancer types (13-16). In the *KRAS*-mutant NSCLC mouse model, the uptake of BCAA by NSCLC cells increased (17).

The second rate-limiting irreversible step of BCAA catabolism is catalyzed by the branched-chain α-keto acid dehydrogenase (BCKDH) complex (18). The branched-chain α-keto acid dehydrogenase kinase (BCKDK) phosphorylates and inactivates the E1α (BCKDHA) subunit of this complex to suppress the catabolism of BCAAs (19). BCKDK regulates BCKDH and adenosine triphosphate (ATP)-citrate lyase, which catalyzes the cleavage of citric acid into oxaloacetate and acetyl-coenzyme A (CoA) (20). BCAAs are strongly associated with dysregulated glucose and lipid metabolism (21). Current research believes that BCKDK is an oncogene. In colorectal cancer, BCKDK promoted tumorigenesis through activation of the MEK/ERK pathway (22). Furthermore, in hepatocellular carcinoma, BCKDK phosphorylation promoted metastasis and proliferation via the ERK signaling pathway (23). However, the importance of BCKDK in regulating the BCAA pool and its impact on NSCLC growth and survival merits investigation.

Here, we identified increased BCAA concomitant with decreased citric acid in the plasma of preoperative NSCLC patients. BCKDK expression was elevated in NSCLC and positively associated with the poor survival of patients. Knockout of BCKDK decreased the proliferation and colony formation of A549 and H1299 cell lines. Furthermore, knockout of BCKDK inhibited glycolysis and promoted oxidative phosphorylation (OXPHOS). Thus, BCKDK may promote tumor progression by regulating glycolysis and tricarboxylic acid (TCA).

We present the following article in accordance with the MDAR reporting checklist (available at https://dx.doi.org/10.21037/tlcr-21-885).

Methods

Participants

This study enrolled 55 patients who presented with histologically confirmed NSCLC at Tianjin Medical University Cancer Institute and Hospital (Tianjin, China) from July 2020 to October 2020. The healthy control group comprised 55 healthy individuals who underwent health screening. Healthy controls showed no abnormalities in blood tests, endoscopic examination, diagnostic imaging, or medical interviews. All procedures performed in this study involving human participants were in accordance with the Declaration of Helsinki (as revised in 2013). The study was approved by ethics board of Tianjin Medical University Cancer Institute and Hospital (No. bc2019114) and informed consent was taken from all the patients.

Fasting blood samples were collected from the patients before and after operation, and blood samples were collected from the patients in the hospital between 8 am and 9 am. Serum was obtained by centrifuging the blood samples at 3,500 rpm for 10 min at 4 ℃. Aliquots of the plasma were stored at −80 ℃ until nuclear magnetic resonance (NMR) spectroscopy was conducted.

Fresh lung cancer tissues and paired adjacent non-tumor lung tissues were obtained from 6 patients who underwent surgery in the Tianjin Medical University Cancer Institute and Hospital between October 2019 and July 2020. None of the patients received any treatment, including radiotherapy or chemotherapy, The stage of lung cancer was determined in accordance with the American Joint Committee on Cancer (AJCC) staging manual, 8th edition.

Detection of metabolites by NMR

Serum samples and cell supernatants were prepared and determined at ProteinT Biotechnology Co. Ltd. (Tianjin, China) in accordance with the Bruker Standard Operating Procedure for In Vitro Diagnostic Studies (IVDr SOP). Briefly, the 300 μL serum sample (thawed at room temperature) was mixed with 300 μL buffer

(phosphate buffer pH 7.4, containing TSP-D4; Bruker Corp, Billerica, MA, USA), and the resulting 600 µL mixture was transferred to a 5 mm NMR tube for analysis. Detection was performed on a 600 MHz NMR Avance III HD spectrometer equipped with a BBI probe and SampleJet autosampler, which was adjusted at 6 ℃ during detection (Bruker Biospin, Rheinstetten, Germany). Each sample was automatically tuned and homogenized prior to collection. Free induction decays were presented in spectral form after Fourier transform and automatically phased and baseline-corrected in Topspin software (Bruker Biospin, Rheinstetten, Germany) as Bruker IVDr. The metabolite concentration is expressed as mmol/L.

Cell lines and culture

The human NSCLC (A549 and H1299) and human embryonic kidney cell line 293T (RRID: CVCL_0063) were purchased from American Type Culture Collection (ATCC; Manassas, VA, USA). 293T cells were grown in Dulbecco's Modified Eagle's Medium (BI, Gaithersburg, MD, USA) supplemented with 10% fetal bovine serum (FBS; Gibco, Waltham, MA, USA). A549 and H1299 cells were cultured in Roswell Park Memorial Institute-1640 (RPMI-1640, BI) supplemented with 10% FBS. All cells were grown at 37 ℃ in a humidified atmosphere with 5% CO_2 and routinely authenticated by observation of growth characteristics and morphology.

Immunohistochemical staining

Paraffin-embedded sections were heated in an incubator at 60 ℃ for 25 min, deparaffinized in xylene, rehydrated using graded alcohol, and endogenous peroxidase quenched using 0.03% H_2O_2. Epitopes were exposed using a 10 mM citrate buffer, microwaved, and then blocked in 10% goat serum. Sections were incubated with rabbit polyclonal anti-BCKDK (Santa Cruz Biotechnology, Inc., Dallas, TX, USA) overnight, followed by incubation with horseradish peroxidase (HRP) secondary antibody (Abcam, Cambridge, UK) and reacted with 3,3'-diaminobenzidine (DAB). After hematoxylin counter-staining, the slides were visualized and imaged under a microscope.

Plasmids, transfection, and generation of stable cell lines

BCKDK knockout (KO) lung cell lines were generated using clustered regularly interspaced short palindromic repeat (CRISPR) genome editing as previously described (24). The BCKDK single guide RNA (sgRNAs) were designed using the CRISPR Design Tool (http://crispr.mit.edu; Zhang Laboratory, Massachusetts Institute of Technology, Cambridge, MA, USA) and purchased from Sangon Biotech (Shanghai, China). The BCKDK knockout plasmid was generated by cloning BCKDK sgRNAs into lenti-CRISPR V2 vectors (Addgene, Watertown, MA, USA). The sgRNA sequences are as follows: 5'-CACCGGCCACCGACACACACCACG-3'; 5'-AAACCGTGGTGTGTGTCGGTGGCC-3'. Lentivirus was produced by co-transfecting 293T cells with BCKDK knockout plasmid and packaging vectors (psPAX2 and pMD2G) using lipo3000 (Invitrogen, Carlsbad, CA, USA). A549 and H1299 cells were infected with virus supernatants with 10 µg/mL polybrene (Solarbio, Beijing, China). At 12 h after the infection, change the medium, continue culturing the cells for 24 h, and then, screen the cells with a complete medium containing puromycin (2 µg/mL) (Sigma-Aldrich, St. Louis, MI, USA) every day for approximately 7 days to obtain a stable cell line. Assays were performed with these stable cell lines.

Western blot

Whole-cell protein was extracted using radioimmunoprecipitation assay lysis buffer (Solarbio, Beijing, China). The cell lysates were incubated on ice for 30 min, and cell debris was removed by centrifugation at 12,000 rpm, 10 min. Protein samples were separated by 8% sodium dodecyl sulfate polyacrylamide gel electrophoresis and then transferred to PVDF membranes (Millipore,USA). The membranes were blocked in 5% skimmed milk for 1 h and then incubated overnight at 4 ℃ with primary antibodies against BCKDK (1:2,000, Santa) and GAPDH (1:5,000, Abcam). After treatment with HRP secondary anti-rabbit or anti-mouse antibodies (Santa Cruz, USA) for 1 h, imaging was performed using Amersham Imager 600 (GE Healthcare, Beijing, China).

Cell proliferation assays

A549 and H1299 cells (1,000 cells per well) were seeded in 96-well plates. After 24 h, each well was mixed with 20 µL of 0.5 mg/mL 3-(4,5-dimethylthiazo-2-yl)-5-(3-carboxymethoxyphenyl)-2-(4-sulfophenyl)-2H-tetrazolium (MTS) reagent (Promega Corp., Madison, WI, USA). The cells were incubated for 1 h, and then the absorbance

was detected at 570 nm on a microplate reader (Bio-Tek Instruments, Winooski, VT, USA). Absorbance values on days 1, 2, 3, 4, and 5 were normalized to the data from day 0 to create a proliferation curve.

For inhibition assays, 2000 A549 and H1299 cells were seeded in 96-well plates for 24 h and then treated with fresh medium containing 200 μM BT2 (allosteric BCKDK inhibitor) for 24 or 48 h. MTS reagents were added to each well at corresponding time points, and then incubation was continued for 1 h. Absorbance was measured at 570 nm.

Colony formation assay

NSCLC cells were seeded into 6-well plates at a density of 500 cells per well, and exposed or not exposed to 200 μM of BT2. The medium was changed every 2 days. After masses of more than 50 cells had accumulated, they were observed under a microscope (Olympus, Tokyo, Japan). The colonies were fixed with paraformaldehyde for at least 1 h, stained with crystal violet for 15 min, photographed, and then counted.

Cell apoptosis

NSCLC cells were seeded into 6-well plates. When 80% confluence was reached, 200 μM of BT2 was added for 24 h. The cell culture supernatant was discarded. Cells of each group were trypsinised and collected, washed twice with 2 mL of 1× PBS on ice, and then resuspended in 1×10^6 cells/mL with 1× buffer. Then, 100 μL of cells (approximately 1×10^5 cells) from each group were added to the flow tube. Each tube was mixed with 5 μL of Annexin V-PE and 5 μL of 7-AAD. The tube wall was flicked by hand to mix the cells, which were then incubated for 15 min at room temperature in the dark. The cells were mixed with 400 μL of 1× buffer, and 1 h of flow cytometry was used for testing.

Analysis of intracellular reactive oxygen species by flow cytometry

NSCLC cells were seeded in a 6-well plate at a density of 4×10^5 cells per well. The next day, the cells were treated with 200 μM of BT2. After treatment, the cells were washed twice with PBS and then incubated with DCFH-DA at a concentration of 5 μM for 10 min at 37 ℃. The cells were subsequently resuspended in PBS. FITC fluorescence was assessed using the BD LSRII flow cytometer and FACSDiva software. Analysis was performed using FlowJo Software (Version X; TreeStar, Ashland, OR, USA).

Oxygen consumption rate (OCR) and extracellular acidification rate measurement (ECAR)

OCR and ECAR were measured using an XF24 Extracellular Flux Analyzer (Seahorse Bioscience, North Billerica, MA, USA). The specific method has been described previously (25). In brief, NSCLC cells were seeded in 24-well plates at a density of 1,000 cells/well and cultured overnight. Then, the temperature and pH are equilibrated, that is, the cells are washed with OCR medium or ECAR medium, and incubated in a CO_2-free incubator at 37 ℃ for 1 h. Operate according to the XF testing procedure. ECAR was measured under baseline conditions and after treatment with glucose (100 mM), oligomycin (100 μM) and 2-deoxyglucose (2-DG; 500 mM). OCR was measured under baseline conditions and after treatment with Oligomycin (100 μM), FCCP (100 μM) and Rotenone/Antimycin (50 μM). Values were normalized to 1×10^4 cell counts. Values are presented as the mean ± standard error.

Determination of extracellular lactate, BCAA, and citrate

Cell culture medium (2 mL) was collected from confluent cells at 24 and 48 h post the corresponding treatment, centrifuged at 1,200 rcf for 5 min and supernatant subjected to NMR spectroscopy.

Statistical analysis

Statistical analyses were performed using SPSS software version 21.0 (IBM Corp., Armonk, NY, USA). Data are reported as the mean ± standard deviation (SD). Biochemical experiments were performed in triplicate, and a minimum of 3 independent experiments was analyzed. Statistical significance of differences was assessed by an unpaired 2-tailed *t*-test and U test. Statistical analyses and data plotting were performed using R software (The R Foundation for Statistical Computing).

Results

The metabolic profile of preoperative NSCLC patients differs from healthy controls

Tumors have distinctive metabolic characteristics compared to healthy tissue. In order to investigate the metabolic

Table 1 Demographics and clinicopathologic characteristics of patients with NSCLC

Characteristics	n=55
Age, mean ± SD, [range], years	55±10 [29–71]
Sex, n (%)	
Male	23 (41.8)
Female	33 (58.2)
TNM stage, n (%)	
IA	53 (96.4)
IB	2 (3.6)
Tumor diameter, n (%)	
≤2 cm	46 (83.6)
>2 cm	9 (16.4)
Pathology type, n (%)	
Squamous cell carcinoma	3 (5.5)
Adenocarcinoma	51 (92.7)
Other	1 (1.8)
KPS performance status, n (%)	
100	39 (70.9)
90	16 (29.1)

NSCLC, non-small cell lung cancer; KPS, Karnofsky Performance Status; TNM, tumor node metastasis.

Table 2 Characteristics of samples from healthy controls (HC)

Characteristics	Value (n=55)
Age, mean ± SD, years	43±10
Sex, n (%)	
Male	26 (47.3)
Female	30 (52.7)

properties of patients with early-stage NSCLC compared to healthy individuals, we collected tumor and blood samples from the two cohorts of patients. A total of 55 NSCLC samples and 55 healthy control patients were included in this study. The mean age of the patients with NSCLC was 55 years, and 41.8% were male. None of the patients received any treatment. Of the total patients, 96.4% were classified as stage 1A and 5.6% as stage 1B in accordance with the AJCC eighth edition. The mean age of the healthy control group was 43 years, and 47.3% were male (*Tables 1*,*2*).

Pairwise comparison was conducted between the healthy controls and the early-stage NSCLC patients to identify distinct biomarkers that may be associated with early-stage NSCLC among thousands of variables. The principal component analysis (PCA) showed a clear separation in serum metabolic phenotypes between the healthy controls and NSCLC patients (*Figure 1A*). Partial least squares-discriminant analysis (PLS-DA) was performed to obtain information between the different groups. The quality of the PLS-DA model was assessed by the R_2Y and Q^2 values, which determined the explanation ability and predictive capacity of the model, respectively (*Figure 1B*). The cumulative R_2Y and Q^2 values were 0.889 and 0.831, respectively. Ten differential metabolic features were obtained using the selection criterion of variable importance in the projection (VIP) >1.0 and P<0.05 from Mann-Whitney-Wilcoxon test with false discovery rate correction. Compared with the healthy control group, the NSCLC group showed higher levels of glutamic acid, formic acid, succinic acid, lactic acid, ornithine, phenylalanine, valine, and BCAAs; and lower levels of glutamine and citric acid (*Table 3*).

The metabolic profile of preoperative NSCLC patients differed from that of postoperative NSCLC patients

In order to confirm that the differential metabolites we detected were indeed caused by tumors and not other factors, we collected blood samples from patients before and after surgery. PCA revealed obvious differences in serum metabolic phenotypes between the pre-and postoperative NSCLC patients (*Figure 2A*). Variables with significantly high VIP (P<0.05) were combined. Eight metabolites were finally identified as differential metabolites, including succinic acid, lactic acid, ornithine, creatine, phenylalanine, and BCAAs, which were all increased; and glutamine and citric acid, which were decreased (*Table 4*). Among the differential metabolic features detected in the serum, six differential metabolites showed a strong overlap. The same pattern of changes was found between healthy versus NSCLC and preoperative NSCLC versus postoperative NSCLC (*Table 5*). The altered metabolites were enriched in five significantly different pathways related to NSCLC (*Figure 2B*). These pathways were strongly associated with amino acids, indicating that the altered amino acids in these pathways have potential as candidate biomarkers for NSCLC.

BCKDK was upregulated in NSCLC and associated with poor prognosis in patients with NSCLC

BCKDK can phosphorylate BCKDHA and ATP citrate

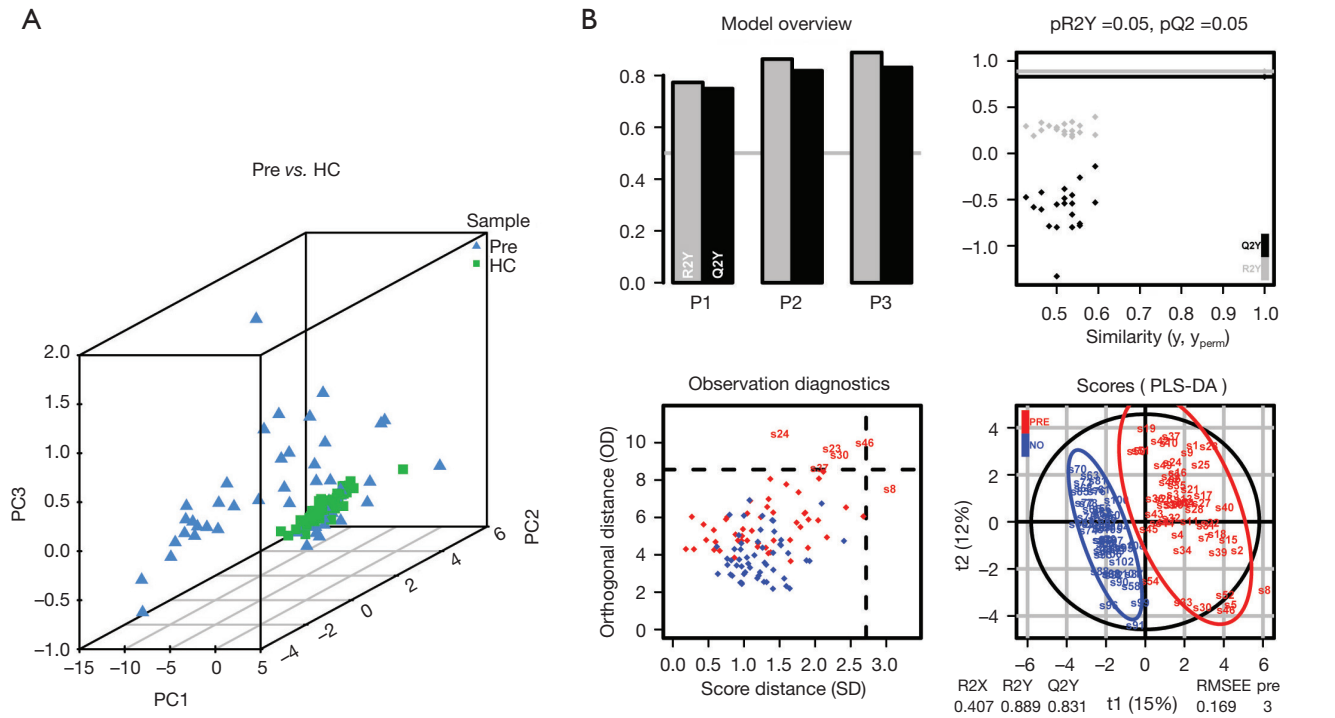

Figure 1 Screening of differential metabolites in the serum of preoperative NSCLC patients differed from healthy controls. (A) A PCA model distinguished the metabolites in the serum of healthy controls and NSCLC patients; (B) score plot, cross validation, and a permutation test of the PLS-DA model for NSCLC patients and healthy controls. NSCLC, non-small cell lung cancer; PCA, principal component analysis; PLS-DA, partial least squares discriminant analysis.

Table 3 Metabolic profiles of preoperative NSCLC patients and healthy controls (PRE *vs.* HC)

Metabolites	PLS-DA (VIP >1)	P	Median (PRE)	Median (HC)	FC (PRE/HC)	Change
Glutamic acid	2.20	<0.001	0.20	0.00	N/A	↑
Formic acid	1.82	<0.001	1.15	0.00	N/A	↑
Succinic acid	1.47	<0.001	0.01	0.00	N/A	↑
Lactic acid	1.87	<0.001	9.40	2.80	3.36	↑
Ornithine	1.18	<0.001	0.07	0.03	2.33	↑
Phenylalanine	1.74	<0.001	0.10	0.05	2.00	↑
Valine	1.05	0.01	0.27	0.24	1.10	↑
BCAA	1.00	0.02	0.44	0.41	1.09	↑
Glutamine	1.97	<0.001	0.51	0.73	0.69	↓
Citric acid	1.31	<0.001	0.10	0.17	0.61	↓

↑, ↓ respectively indicate the increase and decrease of metabolites in the PRE group compared with the HC group. NSCLC, non-small cell lung cancer; BCAA, branched chain amino acids; PRE, preoperative NSCLC patients; PLS-DA, partial least squares discriminant analysis; VIP, variable importance in the projection; HC, healthy controls; FC, fold change.

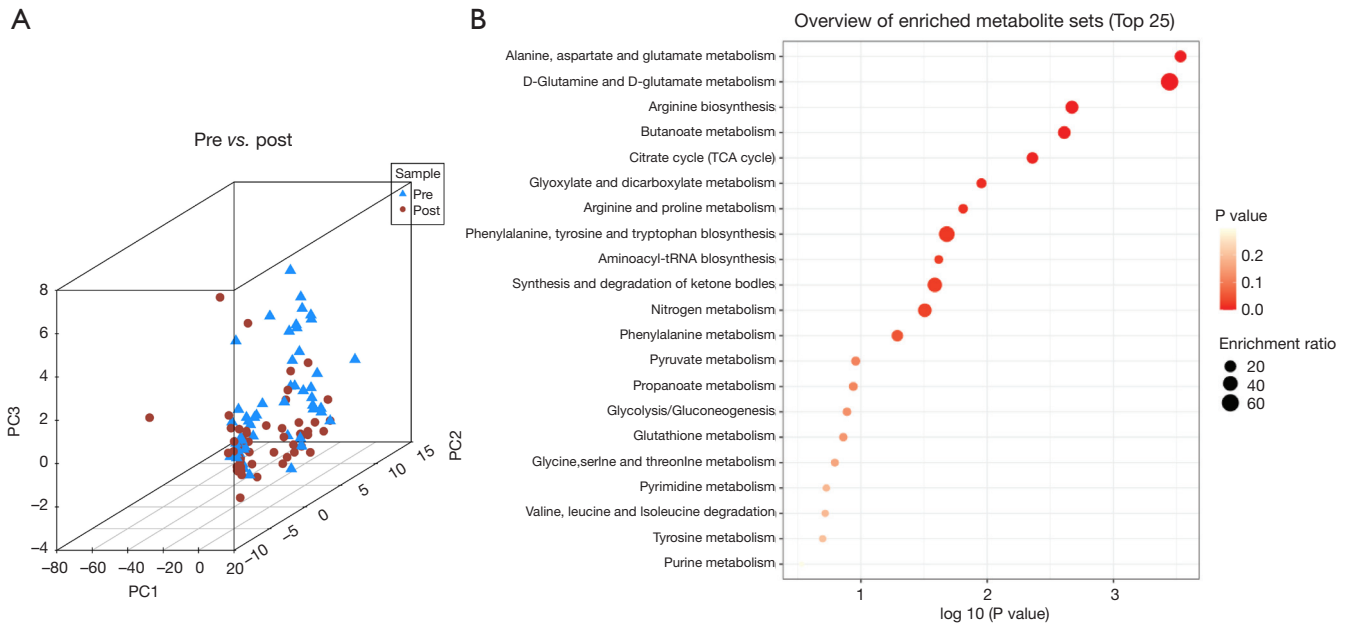

Figure 2 Screening of differential metabolites in the serum of preoperative NSCLC patients differed from that of postoperative NSCLC patients. (A) PCA model distinguished the metabolites detected by NMR in the serum of preoperative NSCLC patients and postoperative NSCLC patients; (B) pathway enrichment analysis of different metabolites. NSCLC, non-small cell lung cancer; PCA, principal component analysis.

lyase (ACLY), exerting opposing effects on both. Compared with the healthy controls and postoperative NSCLC patients, BCAA increased and citrate decreased in the serum of preoperative NSCLC patients (*Figure 3A,3B*). Moreover, BCAA and citrate were not affected by other factors (*Figure 3C,3D*). We hypothesized that patients with NSCLC had an altered metabolism impacted by BCKDK. To investigate this in an independent cohort, the expression levels of *BCKDK*, *BCKDHA*, and *ACLY* in NSCLC and adjacent tissues and their effects on prognosis were examined in The Cancer Genome Atlas (TCGA) database. The expression levels of *BCKDK* and *ACLY* were increased in NSCLC tissue compared to adjacent (*Figure 3E,3F*), with concomitant reduced expression of *BCKDHA* (*Figure 3G*). The prognostic effects of *BCKDK*, *BCKDHA*, and *ACLY* were compared by comparing the overall survival of patients with NSCLC between the low and high expression groups. Results showed that the expression levels of BCKDK, ACLY, and BCKDHA significantly influenced the survival of the patients with NSCLC (*Figure 3H-3J*). Immunohistochemical staining further confirmed BCKDK to be overexpressed in NSCLC tumor tissues (*Figure 3K*). These results indicate that BCKDK is associated with NSCLC and may serve as an indicator of poor prognosis.

Knockout of BCKDK impacts the metabolism of BCAA and citric acid in NSCLC

To further investigate the role of BCKDK in NSCLC BCAA and citric acid metabolism, we knocked-out BCKDK in A549 and H1299 cells by CRISPR genome editing technology. A549-sgNT, A549-sgBCKDK, H1299-sgNT, and H1299-sgBCKDK cell lines were generated (*Figure 4A*). We measured the abundance of BCAA and citrate in the cell culture supernatant with or without knockdown of BCKDK by NMR detection. The content of BCAA was lower and the content of citric acid was higher in the supernatant of the cells with BCKDK knocked out compared to control cells (*Figure 4B,4C*). BT2 is an effective inhibitor of BCKDK (26). Similar to the genetic knockout, the BT2 inhibitor reduced the abundance of BCAA decreased and increased citric acid in both A549 and H1299 cells treated with BT2 (*Figure 4D,4E*).

Knockout of BCKDK attenuates NSCLC proliferation

BCKDK has previously been shown to influence colorectal

Table 4 Metabolic profile of preoperative and postoperative NSCLC patients (PRE *vs.* POST)

Metabolite	PLS-DA (VIP >1)	P	Median (PRE)	Median (POST)	FC (PRE/POST)	Change
Succinic acid	1.58	0.02	0.01	0.00	N/A	↑
Lactic acid	1.43	0.00	9.40	2.80	2.09	↑
Ornithine	1.29	0.04	0.07	0.03	1.75	↑
Creatine	1.24	0.03	0.03	0.03	1.50	↑
Phenylalanine	2.97	<0.001	0.10	0.05	1.43	↑
BCAA	1.17	0.03	0.44	0.41	1.07	↑
Glutamine	1.36	0.02	0.51	0.73	0.91	↓
Citric acid	1.65	0.00	0.10	0.16	0.80	↓

NSCLC, non-small cell lung cancer; BCAA, branched chain amino acids; HC, healthy control; PLS-DA, partial least squares discriminant analysis; VIP, variable importance in the projection; PRE, preoperative NSCLC patients; POST, postoperative NSCLC patients; FC, fold change.

Table 5 Differential metabolites showed overlap and the same pattern of change between healthy versus NSCLC patients and preoperative NSCLC versus postoperative NSCLC patients

Metabolite	PRE *vs.* HC		PRE *vs.* POST	
	FC	P value	FC	P value
Glutamine	0.69	<0.001	0.91	0.02
Phenylalanine	2.00	<0.001	1.43	<0.001
Citric acid	0.61	<0.001	0.80	0.00
Lactic acid	3.36	<0.001	2.09	0.00
Ornithine	2.33	<0.001	1.75	0.04
BCAA	1.09	0.02	1.07	0.03
Succinic acid	NA	<0.001	NA	0.02

NSCLC, non-small cell lung cancer; BCAA, branched chain amino acids; HC, healthy control; PRE, preoperative NSCLC patients; POST, postoperative NSCLC patients; FC, fold change.

cancer progression in a BCAA-independent manner (22), while citrate exerts an antiproliferative effect (27). The growth curves of A549-sgNT and A549-sgBCKDK cells or H1299-sgNT and H1299-sgBCKDK cells were compared to test whether BCKDK promotes cell proliferation in NSCLC cells. Results showed that the growth of A549-sgBCKDK and H1299-sgBCKDK cells was slower than that of A549-sgNT and H1299-Mock cells (*Figure 5A,5B*). Similar results were observed in the cells treated with BT2 (*Figure 5C,5D*). The anchorage-independent growth was next compared. The number of sgBCKDK (BT2) colonies was considerably lower than that of sgNT (DMSO) (*Figure 5E,5F*). In addition, BT2 and BCKDK knockout resulted in enhanced cell apoptosis (*Figure 5G,5H*). These results indicate that BCKDK Inhibit apoptosis of NSCLC cells.

BCKDK protect the NSCLC cells from apoptosis by maintaining glycolysis and ROS

Glycolytic metabolism is critical in cancer cells to facilitate proliferation and fast energy production (28). BCKDK plays an important role in BCAA and citrate degradation, key factors in this process. Thus, glycolysis and oxidative respiration pathway activity was investigated in BCKDK knockout NSCLC cells. The oxidative consumption rate (OCR) was analyzed in NSCLC after treatment with oligomycin, p-trifluoromethoxy carbonyl cyanide

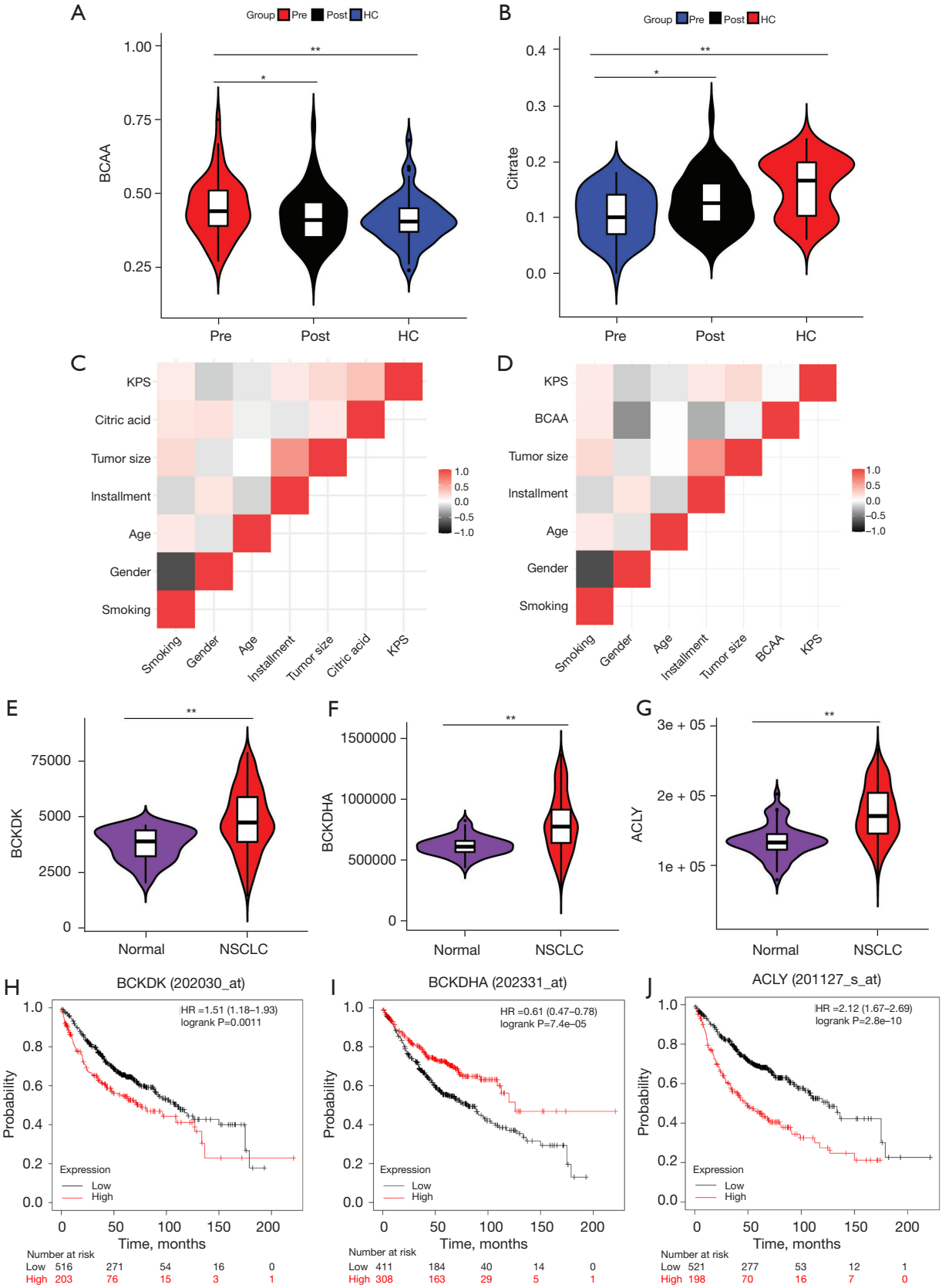

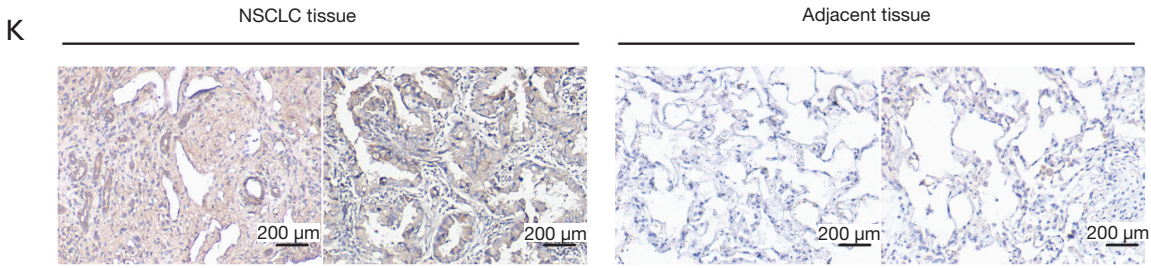

BCKDK expression in NSCLC

	Cancer tissue	Adjacent tissue	P value
Positive rate	82%	41%	<0.001
Staining strength	3.7+	1.8+	<0.01

Figure 3 BCKDK is upregulated in NSCLC and associated with poor prognosis of patients with NSCLC. Serum levels of BCAA (A) and citrate (B) in healthy controls and NSCLC patients. Correlation of BCAA (C) and citrate (D) with other clinical indicators. The expression levels of BCKDK (E), BCKDHA (F), and ACLY(G) in NSCLC tissue were measured using TCGA database. (H-J) The expression levels of BCKDK, BCKDHA, and ACLY in NSCLC tissue were measured using the KM-Plot database. (K) IHC staining of BCKDK in NSCLC. Representative images are shown (×200, scale bar =40 μm). *, P<0.05; **, P<0.01. BCAA, branched chain amino acids; ACLY, ATP citrate lyase; BCKDK, branched chain keto acid dehydrogenase kinase; BCKDHA, BCKDK phosphorylates and inactivates the E1α; TCGA, The Cancer Genome Atlas; IHC, immunohistochemistry; NSCLC, non-small cell lung cancer.

phenylhydrazone, and antimycin A, using the Seahorse Flux analyzer. BCKDK knockout increased the OCR in both A549 and H1299 cells (*Figure 6A,6B*). The glycolytic extracellular acidification rate (ECAR) was also calculated after serial treatment of glucose, oligomycin, and 2-deoxyglucose. Conversely to the increased oxidative respiration rate, ECAR was remarkably decreased in A549-sgBCKDK and H1299-sgBCKDK cells (*Figure 6C,6D*). BT2 also increased OCR and decreased ECAR in A549 and H1299 cells (*Figure 6E-6H*). Extracellular glucose analysis suggested that BCKDK knockout inhibited glucose consumption in A549 and H1299 cells (*Figure 6I*). The level of extracellular lactate was also measured as an agent indicator of glycolysis, and showed a significant decrease in A549 and H1299 cells with BCKDK knockout (*Figure 6J*) or inhibition (*Figure 6K,6L*). Furthermore, by assessing reactive oxygen species (ROS) in the cells, we find a significant increase with BCKDK knockout or inhibition in A549 and H1299 cells (*Figure 6M,6N*).

Discussion

Cellular metabolic reprogramming is a common and important feature observed in cancer. Several studies in recent years have analyzed tumor-related metabolic markers, including sugars, lipids, and amino acids, by detecting the body fluids of patients with tumors (29-31). However, the mechanism of metabolic changes and their impact on the development and progression of cancer remain poorly understood (13). Our study revealed that six metabolites in plasma samples of preoperative NSCLC patients were significantly altered compared with healthy controls and postoperative NSCLC patients. Glutamine, phenylalanine, citric acid, lactic acid, ornithine, and BCAAs showed significant changes before and after surgery in patients with NSCLC, suggesting their association with tumor metabolism. BCKDK, the upstream kinase that regulates BCKDHA and ACLY, was highly expressed in NSCLC tumor tissue and was associated with poor prognosis. The role of BCKDH complex and BCAT subtypes (BCAT1 and BCAT2) has been widely explored in different cancers, but the role of BCKDK is limited and has not been reported in NSCLC. Our data show that knockout of BCKDK in NSCLC cell lines A549 and H1299 inhibited glycolysis, increased ROS generation, and increased cell death. These results suggest that BCKDK regulates cellular metabolism which directly impacts cell survival.

Since the discovery of the Warburg effect, many rate-limiting enzymes involved in glucose and lipid metabolism have become the focus of tumor metabolism research. These enzymes include hexokinase-2, pyruvate kinase M2 (32), isocitrate hydrogenase (33), and ACLY (34), which are

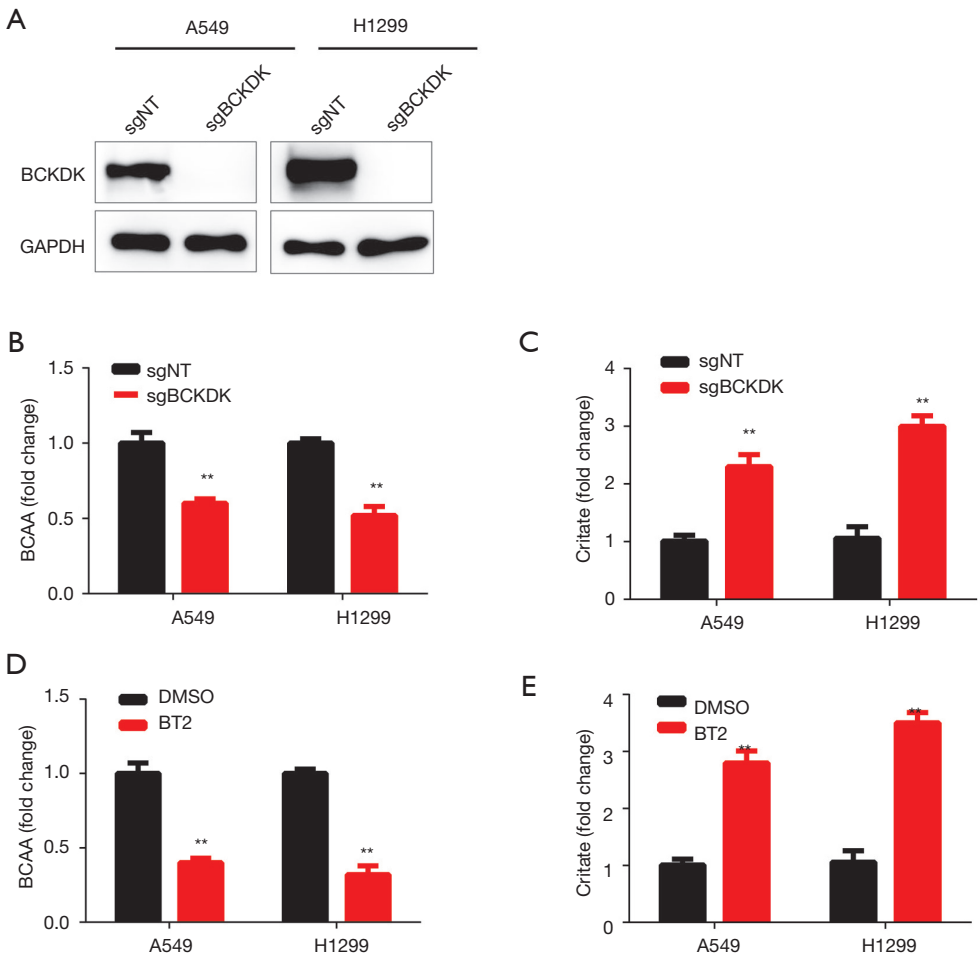

Figure 4 BCKDK affected the metabolism of BCAA and citric acid in NSCLC cell lines. (A,B) CRISPR-Cas9 was used to knock out BCKDK expression in A549 and H1299 cells. Knockout efficiency was confirmed through western blot and qRT-PCR; (C,D) knocking out BCKDK increased BCAA and decreased citrate in A549 and 1299 cell lines; (E,F) inhibiting BCKDK with BT2 increased BCAA and decreased citrate in A549 and H1299 cell lines. The data are presented as the mean ± SD of 2 replications. **, P<0.01. BCAA, branched chain amino acids; BCKDK, branched chain keto acid dehydrogenase kinase.

potential targets for cancer therapy. Amino acid metabolism is also closely related to tumor development (35). Glutamine is an abundant nonessential amino acid in the bloodstream. In addition to glucose, proliferating cancer cells also rely on glutamine for energy and basic sustenance (36). Many clinical studies have demonstrated that serum glutamine levels are lower in cancer patients compared with healthy controls, with the level being related to tumor stage and prognosis (37-39), and the present study results are consistent with this. *In vitro* experiments have shown that the inhibition of glutaminase, a key enzyme for glutamine metabolism, significantly reduces cell viability (40). Elevated levels of BCAA in plasma and tumor tissues have been observed in many types of human cancers, including hepatocellular carcinoma (HCC) (15), breast cancer (41), leukemia (13), early pancreatic ductal adenocarcinoma (PDAC) (42) and renal clear cell carcinoma (43). In one study, the reprogramming of BCAA metabolism was determined by changing the expression and activity of BCAA transporters and metabolic enzymes involved in the BCAA metabolic pathway, suggesting branched chain amino acid transaminase 1 (BCAT1) catalyzes the reformation of BCKA through the blood circulation, allowing these cancer cells to accumulate BCAAs (13). Results of the present study showed that BCAAs increased in the plasma of patients with NSCLC. This phenomenon may be related to the

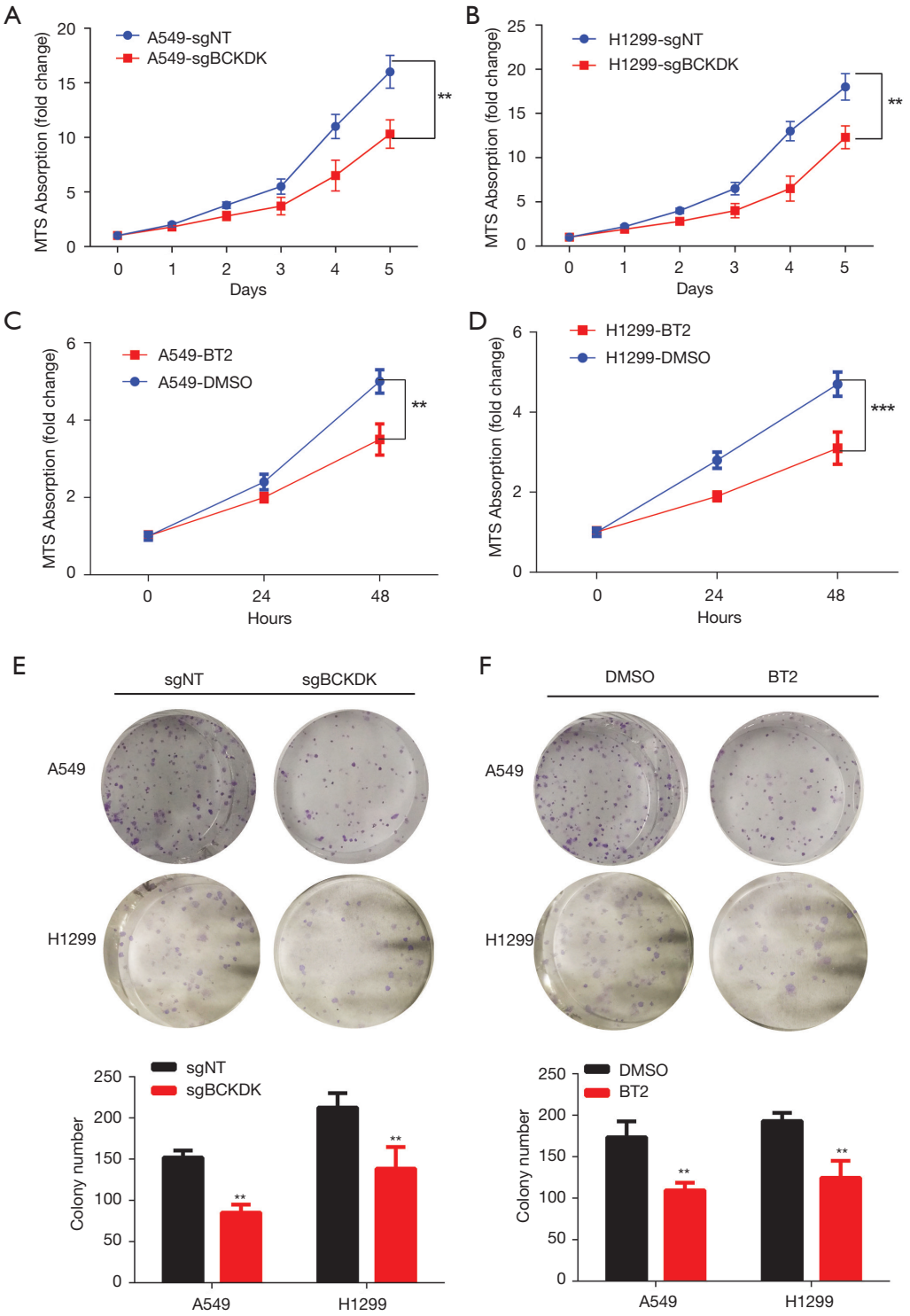

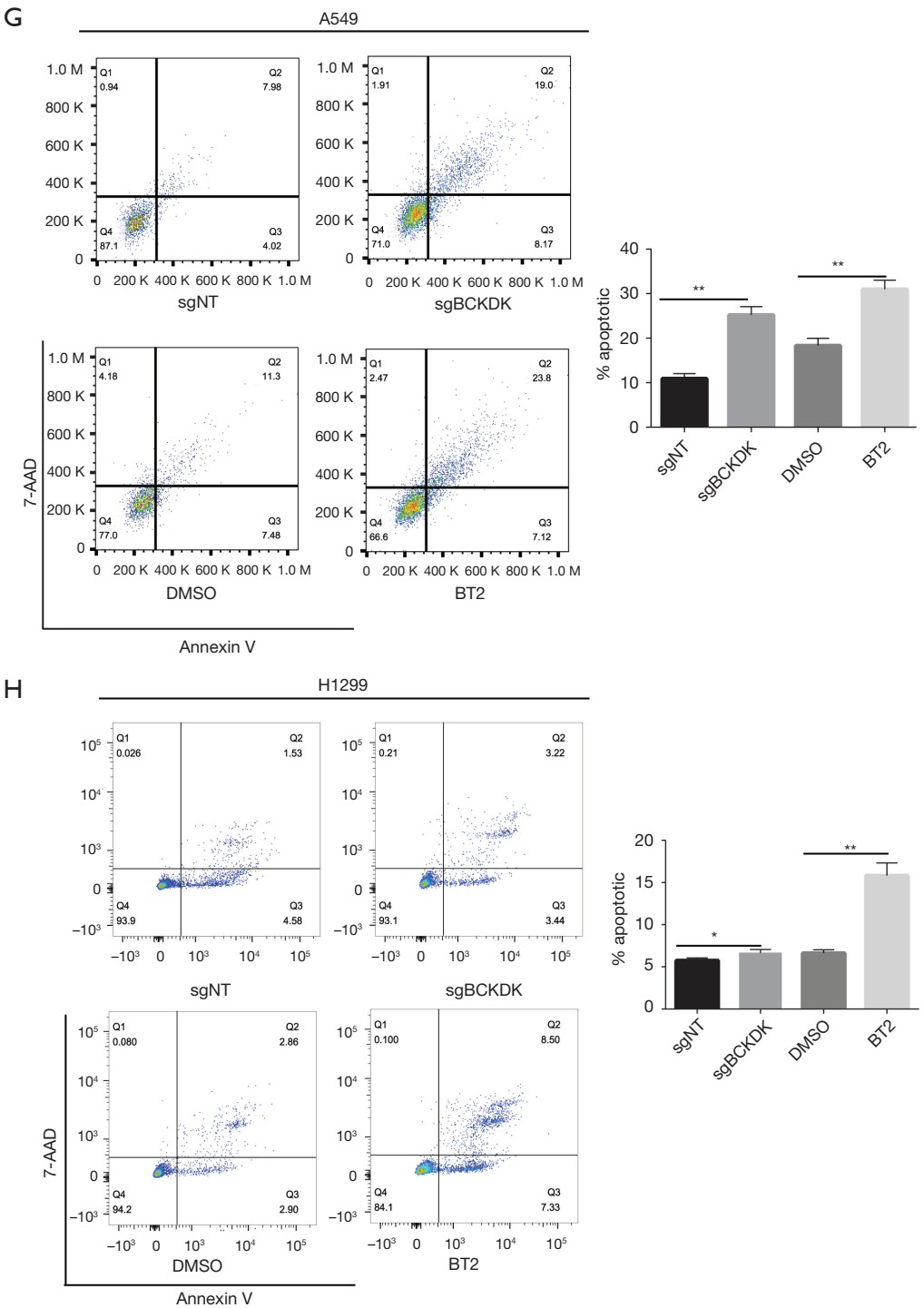

Figure 5 BCKDK promoted the proliferation of NSCLC cells. (A,B) A549 and H1299 cells infected with sgBCKDK or sgNT were assessed by MTS assay, and those treated with BT2 were assessed by MTS assay (C,D). (E,F) Crystal violet staining was used to detect the formation of A549 andH1299 clones after transfection or BT2 treatment. The experiment was repeated three times; (G) A549 and (H) H1299 cells infected with sgBCKDK or BT2 were assessed by apoptosis analysis. Data are presented as the mean ± SD of 3 replications. *, P<0.05; **, P<0.01; ***, P<0.001. MTS, 3-(4,5-dimethylthiazol-2-yl)-5-(3-carboxymethoxyphenyl)-2-(4-sulfophenyl)-2H-tetrazolium; BCKDK, branched chain keto acid dehydrogenase kinase.

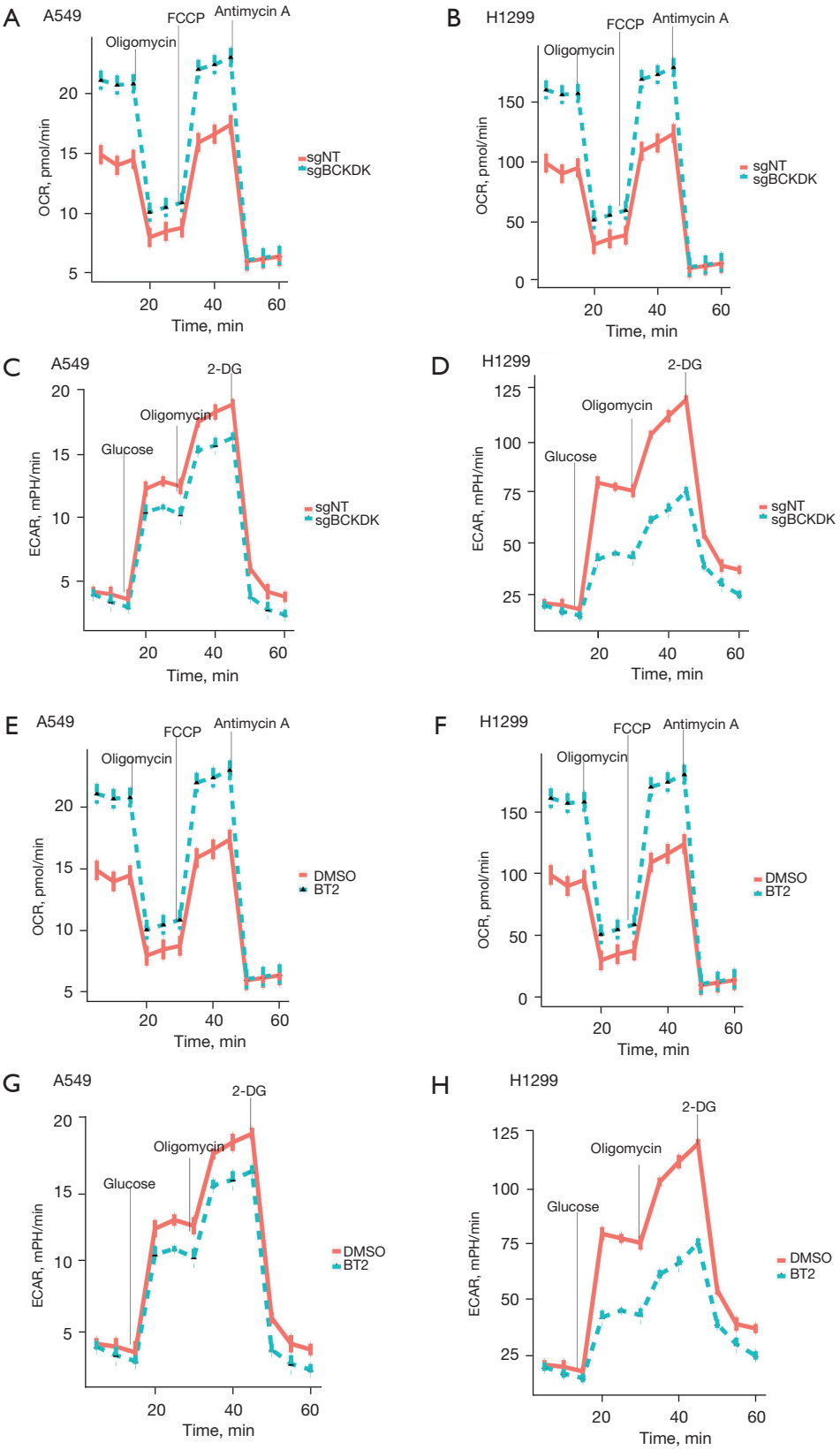

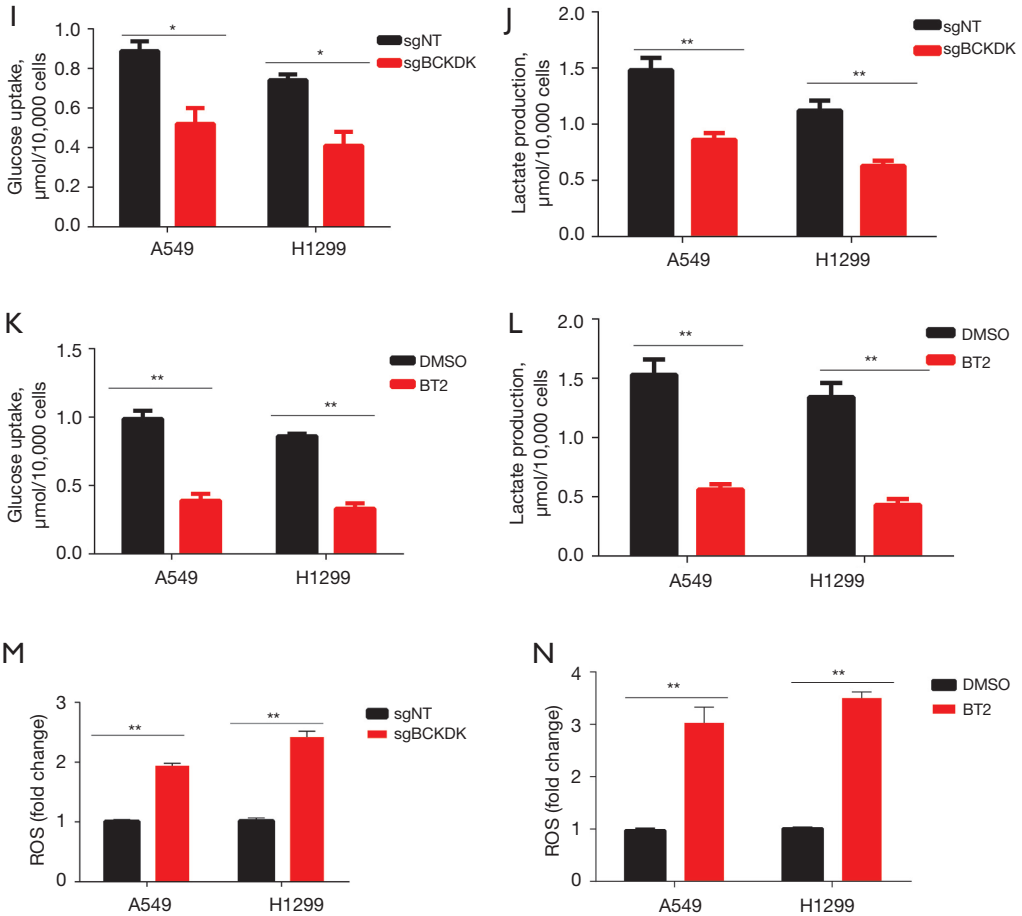

Figure 6 BCKDK suppressed glycolysis and enhanced oxidative phosphorylation in NSCLC. (A-D) OCR and ECAR were assessed in A549 and H1299 cells infected with sgBCKDK or sgNT. (E-H) OCR and ECAR were assessed in A549 and H1299 cells treated with BT2. (I,J) A549 and H1299 cells infected with sgBCKDK or sgNT. Then, glucose uptake and lactate production were measured over the subsequent 36 h. (K,L) A549 and H1299 cells were treated with BT2. Then, glucose uptake and lactate production were measured over the subsequent 36 h. (M,N) A549 and H1299 cells were infected with sgBCKDK or sgNT or treated with BT2. Then, the ROS were measured. Data are presented as the mean ± SD of 3 replications. *, P<0.05; **, P<0.01. BCKDK, branched-chain α-keto acid dehydrogenase kinase; ROS, reactive oxygen species; OCR, oxygen consumption rate; ECAR, extracellular acidification rate.

decreased expression of BCAT1/2 and BCKDH and the increased expression of BCKDK in patients with NSCLC. Using a *KRAS* mutant NSCLC mouse model, Mayers *et al.* reported that the level of plasma BCAA decreases while the expression levels of BCAT1 and pBCKDH increase (44).

BCAA metabolism is strictly regulated by BCKDK and PPM2C (45). Fibroblasts lacking BCKDK feature mitochondrial fusion and fission disorders, increased superoxide anion production, decreased ATP synthesis, and cell cycle arrest (46). BCKA accumulation caused by BCAA catabolism defects may directly inhibit the TCA cycle and mitochondrial oxidative phosphorylation in liver mitochondria. In Kaufman oculocerebrofacial syndrome, BCKDK is a substrate of UBE3B, a ubiquitin ligase. A plasma and cortical metabolome analysis of *Ube3b*$^{-/-}$ mice showed that nucleotide metabolism and TCA cycle are disturbed (17). In this study, knockout of BCKDK was associated with an increase in OCR and ROS in A549 and H1299 cells. This result suggests that BCKDK is a key molecule that regulates the function of cell mitochondria.

ACLY is the hub that links sugar metabolism, lipid metabolism, and amino acid metabolism, and is highly expressed in different tumors (32). Except for prostate cancer, citric acid levels are lower in the serum of tumor

patients, which may be related to the high expression of ACLY. Phosphofructokinase 1 (PFK1), the key enzyme regulating glycolytic flux, can be inhibited by citric acid. High ACLY activity prevents the negative feedback caused by ATP and citric acid to PFK1, thereby promoting glycolysis (47). BCKDK can activate ACLY and promote the cleavage of citric acid into acetyl-CoA, and oxaloacetate. Recent studies have reported that BCKDK can inactivate the phosphorylation of pyruvate dehydrogenase complex to prevent pyruvate from entering the TCA cycle (48). The above research can partly explain why BCKDK knockout inhibited the glycolysis of A549 and H1299 in our study. Thus, BCKDK is a key molecule that affects cell metabolism.

BCKDK promotes the occurrence of colorectal cancer through the MAPK/ERK signaling pathway, and knocking down BCKDK inhibits the metastasis and invasion of colorectal cancer (21,49). In liver cancer, phosphorylated BCKDK promotes cell proliferation and metastasis through the ERK signaling pathway (22). The present findings confirm these studies in NSCLC, by knocking out BCKDK. Whether or not this phenomenon is driven by metabolic changes, activation of signaling pathways, or a combination of the two, warrants further investigation.

Since BCKDK has been found to enhance MAPK/ERK signaling, a key pathway driving cell growth and proliferation in many cancers, it has become an attractive therapeutic target. The most commonly used allosteric BCKDK inhibitor is BT2 (as used in our study) was identified by high-throughput screening. BT2 has an IC_{50} of 3.2 μM with a good *in vitro* stability ($t_{1/2}$ >240 min) (50). Although no BCKDK inhibitor is under clinical evaluation yet, the search for small molecule allosteric inhibitors in ongoing an optimizing of these inhibitors might form the basis for future drug candidates for the treatment of BCKDK-driven malignancies.

In summary, we have demonstrated that BCKDK can promote NSCLC proliferation and can be reversed *in vitro* by the allosteric BCKDK inhibitor BT2, a finding that, if confirmed, may have clinical implications for the future treatment of NSCLC patients.

Acknowledgments

The authors appreciate the academic support from the AME Lung Cancer Collaborative Group.

Funding: This work was supported by the National Natural Science Foundation of China (81802432), CSCO-Merck Serono Oncology Research Fund (Y-MX2015-092) and Tianjin Science Foundation (20JCYBJC00100).

Footnote

Reporting Checklist: The authors have completed the MDAR reporting checklist. Available at https://dx.doi.org/10.21037/tlcr-21-885

Data Sharing Statement: Available at https://dx.doi.org/10.21037/tlcr-21-885

Conflicts of Interest: All authors have completed the ICMJE uniform disclosure form (available at https://dx.doi.org/10.21037/tlcr-21-885). The authors have no conflicts of interest to declare.

Ethical Statement: The authors are accountable for all aspects of the work in ensuring that questions related to the accuracy or integrity of any part of the work are appropriately investigated and resolved. All procedures performed in this study involving human participants were in accordance with the Declaration of Helsinki (as revised in 2013). The study was approved by ethics board of Tianjin Medical University Cancer Institute and Hospital (No. bc2019114) and informed consent was taken from all the patients.

References

1. Siegel RL, Miller KD, Jemal A. Cancer statistics, 2020. CA Cancer J Clin 2020;70:7-30.
2. Sun D, Li H, Cao M, et al. Cancer burden in China: trends, risk factors and prevention. Cancer Biol Med 2020;17:879-95.
3. Gill KS, Fernandes P, O'Donovan TR, et al. Glycolysis inhibition as a cancer treatment and its role in an anti-tumour immune response. Biochim Biophys Acta 2016;1866:87-105.
4. Hu C, Liu Z, Zhao H, et al. A biochemical comparison

of the lung, colonic, brain, renal, and ovarian cancer cell lines using 1H-NMR spectroscopy. Biosci Rep 2020;40:BSR20194027.
5. Hao D, Sengupta A, Ding K, et al. Metabolites as Prognostic Markers for Metastatic Non-Small Cell Lung Cancer (NSCLC) Patients Treated with First-Line Platinum-Doublet Chemotherapy. Cancers (Basel) 2020;12:1926.
6. Tian Y, Wang Z, Liu X, et al. Prediction of Chemotherapeutic Efficacy in Non-Small Cell Lung Cancer by Serum Metabolomic Profiling. Clin Cancer Res 2018;24:2100-9.
7. Chen Y, Lin D, Chen Z, et al. Revealing different lung metastatic potentials induced metabolic alterations of hepatocellular carcinoma cells via proton nuclear magnetic resonance spectroscopy. J Cancer 2018;9:4696-705.
8. Hu JM, Sun HT. Serum proton NMR metabolomics analysis of human lung cancer following microwave ablation. Radiat Oncol 2018;13:40.
9. Padayachee T, Khamiakova T, Louis E, et al. The impact of the method of extracting metabolic signal from 1H-NMR data on the classification of samples: A case study of binning and BATMAN in lung cancer. PLoS One 2019;14:e0211854.
10. Enko D, Moro T, Holasek S, et al. Branched-chain amino acids are linked with iron me-tabolism. Ann Transl Med 2020;8:1569.
11. Rivera ME, Lyon ES, Johnson MA, et al. Effect of valine on myotube insulin sensitivity and metabolism with and without insulin resistance. Mol Cell Biochem 2020;468:169-83.
12. Mochel F, Charles P, Seguin F, et al. Early energy deficit in Huntington disease: identification of a plasma biomarker traceable during disease progression. PLoS One 2007;2:e647.
13. Hattori A, Tsunoda M, Konuma T, et al. Cancer progression by reprogrammed BCAA metabolism in myeloid leukaemia. Nature 2017;545:500-4.
14. Lei MZ, Li XX, Zhang Y, et al. Acetylation promotes BCAT2 degradation to suppress BCAA catabolism and pancreatic cancer growth. Signal Transduct Target Ther 2020;5:70.
15. Ericksen RE, Lim SL, McDonnell E, et al. Loss of BCAA Catabolism during Carcinogenesis Enhances mTORC1 Activity and Promotes Tumor Development and Progression. Cell Metab 2019;29:1151-1165.e6.
16. Wang P, Wu S, Zeng X, et al. BCAT1 promotes proliferation of endometrial cancer cells through reprogrammed BCAA metabolism. Int J Clin Exp Pathol 2018;11:5536-46.
17. Mayers JR, Torrence ME, Danai LV, et al. Tissue of origin dictates branched-chain amino acid metabolism in mutant Kras-driven cancers. Science 2016;353:1161-5.
18. Harris RA, Joshi M, Jeoung NH, et al. Overview of the molecular and biochemical basis of branched-chain amino acid catabolism. J Nutr 2005;135:1527S-30S.
19. Suryawan A, Hawes JW, Harris RA, et al. A molecular model of human branched-chain amino acid metabolism. Am J Clin Nutr 1998;68:72-81.
20. White PJ, McGarrah RW, Grimsrud PA, et al. The BCKDH Kinase and Phosphatase Integrate BCAA and Lipid Metabolism via Regulation of ATP-Citrate Lyase. Cell Metab 2018;27:1281-1293.e7.
21. Lee JH, Cho YR, Kim JH, et al. Branched-chain amino acids sustain pancreatic cancer growth by regulating lipid metabolism. Exp Mol Med 2019;51:1-11.
22. Xue P, Zeng F, Duan Q, et al. BCKDK of BCAA Catabolism Cross-talking With the MAPK Pathway Promotes Tumorigenesis of Colorectal Cancer. EBioMedicine 2017;20:50-60.
23. Zhai M, Yang Z, Zhang C, et al. APN-mediated phosphorylation of BCKDK promotes hepatocellular carcinoma metastasis and proliferation via the ERK signaling pathway. Cell Death Dis 2020;11:396.
24. Sanjana NE, Shalem O, Zhang F. Improved vectors and genome-wide libraries for CRISPR screening. Nat Methods 2014;11:783-4.
25. Zhou M, Shao J, Wu CY, et al. Targeting BCAA Catabolism to Treat Obesity-Associated Insulin Resistance. Diabetes 2019;68:1730-46.
26. Uddin GM, Zhang L, Shah S, et al. Impaired branched chain amino acid oxidation contributes to cardiac insulin resistance in heart failure. Cardiovasc Diabetol. 2019;18:86.
27. Icard P, Lincet H. The reduced concentration of citrate in cancer cells: An indicator of cancer aggressiveness and a possible therapeutic target. Drug Resist Updat 2016;29:47-53.
28. Liberti MV, Locasale JW. The Warburg Effect: How Does it Benefit Cancer Cells? Trends Biochem Sci 2016;41:211-8.
29. Yang B, Ren N, Guo B, et al. Measuring serum human epididymis secretory protein au-toantibody as an early biomarker of lung cancer. Transl Cancer Res 2020;9:735-41.
30. Widlak P, Pietrowska M, Polanska J, et al. Serum mass profile signature as a biomarker of early lung cancer. Lung Cancer 2016;99:46-52.

31. Chae YK, Kim WB, Davis AA, et al. Mass spectrometry-based serum proteomic signa-ture as a potential biomarker for survival in patients with non-small cell lung cancer re-ceiving immunotherapy. Transl Lung Cancer Res 2020;9:1015-28.
32. Patra KC, Wang Q, Bhaskar PT, et al. Hexokinase 2 is required for tumor initiation and maintenance and its systemic deletion is therapeutic in mouse models of cancer. Cancer Cell 2013;24:213-28.
33. Bendahou MA, Arrouchi H, Lakhlili W, et al. Computational Analysis of IDH1, IDH2, and TP53 Mutations in Low-Grade Gliomas Including Oligodendrogliomas and Astrocytomas. Cancer Inform 2020;19:1176935120915839.
34. Icard P, Wu Z, Fournel L, et al. ATP citrate lyase: A central metabolic enzyme in cancer. Cancer Lett 2020;471:125-34.
35. Ananieva EA, Wilkinson AC. Branched-chain amino acid metabolism in cancer. Curr Opin Clin Nutr Metab Care 2018;21:64-70.
36. Li T, Le A. Glutamine Metabolism in Cancer. Adv Exp Med Biol 2018;1063:13-32.
37. Ling HH, Pan YP, Fan CW, et al. Clinical Significance of Serum Glutamine Level in Patients with Colorectal Cancer. Nutrients 2019;11:898.
38. Kumar N, Shahjaman M, Mollah MNH, et al. Serum and Plasma Metabolomic Biomarkers for Lung Cancer. Bioinformation 2017;13:202-8.
39. Xiong Y, Shi C, Zhong F, et al. LC-MS/MS and SWATH based serum metabolomics enables biomarker discovery in pancreatic cancer. Clin Chim Acta 2020;506:214-21.
40. Kodama M, Oshikawa K, Shimizu H, et al. A shift in glutamine nitrogen metabolism contributes to the malignant progression of cancer. Nat Commun 2020;11:1320.
41. Zhang L, Han J. Branched-chain amino acid transaminase 1 (BCAT1) promotes the growth of breast cancer cells through improving mTOR-mediated mitochondrial biogenesis and function. Biochem Biophys Res Commun 2017;486:224-31.
42. Mayers JR, Wu C, Clish CB, et al. Elevation of circulating branched-chain amino acids is an early event in human pancreatic adenocarcinoma development. Nat Med 2014;20:1193-8.
43. Qu YY, Zhao R, Zhang HL, et al. Inactivation of the AMPK-GATA3-ECHS1 Pathway Induces Fatty Acid Synthesis That Promotes Clear Cell Renal Cell Carcinoma Growth. Cancer Res 2020;80:319-33.
44. Peng H, Wang Y, Luo W. Multifaceted role of branched-chain amino acid metabolism in cancer. Oncogene 2020;39:6747-56.
45. Oyarzabal A, Bravo-Alonso I, Sánchez-Aragó M, et al. Mitochondrial response to the BCKDK-deficiency: Some clues to understand the positive dietary response in this form of autism. Biochim Biophys Acta 2016;1862:592-600.
46. Cheon S, Kaur K, Nijem N, et al. The ubiquitin ligase UBE3B, disrupted in intellectual disability and absent speech, regulates metabolic pathways by targeting BCKDK. Proc Natl Acad Sci U S A 2019;116:3662-7.
47. Granchi C. ATP citrate lyase (ACLY) inhibitors: An anti-cancer strategy at the crossroads of glucose and lipid metabolism. Eur J Med Chem 2018;157:1276-91.
48. Heinemann-Yerushalmi L, Bentovim L, Felsenthal N, et al. BCKDK regulates the TCA cycle through PDC in the absence of PDK family during embryonic development. Dev Cell 2021;56:1182-1194.e6.
49. Tian Q, Yuan P, Quan C, et al. Phosphorylation of BCKDK of BCAA catabolism at Y246 by Src promotes metastasis of colorectal cancer. Oncogene 2020;39:3980-96.
50. Tso SC, Gui WJ, Wu CY, et al. Benzothiophene carboxylate derivatives as novel allosteric inhibitors of branched-chain α-ketoacid dehydrogenase kinase. J Biol Chem 2014;289:20583-93.

(English Language Editor: J. Gray)

Cite this article as: Wang Y, Xiao J, Jiang W, Zuo D, Wang X, Jin Y, Qiao L, An H, Yang L, Dumoulin DW, Dempke WCM, Best SA, Ren L. BCKDK alters the metabolism of non-small cell lung cancer. Transl Lung Cancer Res 2021;10(12):4459-4476. doi: 10.21037/tlcr-21-885

